High-mobility window for two-dimensional electron gases at ultrathin AlN/GaN heterojunctions

Yu Cao[a] and Debdeep Jena
Department of Electrical Engineering, University of Notre Dame, Indiana, 46556

(Received 9 March 2007; accepted 9 April 2007; published online 2 May 2007)

High-conductivity two-dimensional electron gases at AlN/GaN heterojunctions are reported. The sheet densities can be tuned from $\sim 5\times 10^{12}/\mathrm{cm}^2$ to $\sim 5\times 10^{13}/\mathrm{cm}^2$ by varying the AlN thickness from 2 to 7 nm. A critical thickness is observed beyond which biaxial strain relaxation and cracking of AlN occur, and a degradation of carrier mobility is seen to occur at extremely high sheet densities. A high-mobility window is identified, within which room-temperature mobility exceeding 1000 $\mathrm{cm}^2/\mathrm{V\,s}$. and sheet densities in the $(1-3)\times 10^{13}/\mathrm{cm}^2$ are obtained, yielding record low sheet resistances in the range of $\sim 170\ \Omega/\square$. Interface roughness scattering and strain relaxation are identified as the factors preventing lower sheet resistances at present. © *2007 American Institute of Physics*. [DOI: 10.1063/1.2736207]

Ultrathin AlN layers grown on GaN have been of great interest recently for a number of applications. AlN layers, when inserted at strained AlGaN/GaN and lattice-matched AlInN/GaN heterojunctions, have been observed to improve the mobility of two-dimensional electron gases (2DEGs) by removing alloy scattering.[1,2] Owing to the large conduction band offset between AlN and GaN, the high-field characteristics of high-electron-mobility transistors (HEMTs) are also improved due to the prevention of real-space transfer of electrons from the channel into the barrier region and/or higher satellite valleys in the barrier which have lower effective masses. In addition to obvious applications in high transconductance, low threshold voltage HEMTs,[3–5] the high-density, high-mobility 2DEGs at ultrashallow *single* AlN/GaN heterojunctions can enable a variety of devices such as high-performance transparent biosensors, plasma-wave terahertz emitters, and other applications where a highly conductive channel buried a few nanometers under the surface is desirable. AlN/GaN superlattices can be used for intersubband infrared detectors and, if the period is sufficiently short so as to form minibands, can be used as "digital alloys" for enhancing the vertical carrier transport for both electrons and holes in ultraviolet emitters and detectors.[6]

Few reports exist on the growth of ultrashallow (few nanometers) pseudomorphic single AlN/GaN heterojunctions.[4,7–9] Strain relaxation in AlN/GaN structures has been studied by some groups.[10–13] The deterioration of the transport properties caused by such relaxation in AlN/GaN (Refs. 8 and 12) has also been reported. However, a *systematic* study of the dependence of the critical AlN thickness, the 2DEG sheet density, and mobility on the thickness of the AlN barrier layer is still lacking. In light of the many applications outlined, such a systematic study is highly desirable and is the subject of this letter.

All growths of the AlN/GaN heterojunctions studied here were performed by molecular beam epitaxy in a Veeco Gen 930 system on semi-insulating GaN templates on sapphire. All growths were performed under metal rich conditions, with the Ga flux of $\sim 10^{-7}$ torr for the GaN layers and the Al flux of $\sim 4\times 10^{-8}$ torr for the AlN layers. The Ga shutter was kept open during the growth of AlN layers to enhance the diffusivity of Al adatoms on the surface. Both the GaN buffer layers and the AlN layers were grown at 800 °C. Active N_2 was supplied through a Veeco rf source, with a plasma power of 150 W. The structures comprised of an ~143-nm-thick undoped GaN buffer layer, followed by an ultrathin AlN cap, the thickness of which was varied between 1.0 and 8.0 nm. The growth rate was measured to be 86.4 nm/h—it was calibrated by a high-resolution x-ray diffraction measurement for a nine-period 4.6 nm/56.0 nm AlN/GaN multiple quantum well calibration structure. The thicknesses and the growth rate were calibrated by fitting the measured data to a simulation. A Hall measurement of this calibration sample yielded a mobility of $\sim 1200\ \mathrm{cm}^2/\mathrm{V\,s}$ at room temperature and $\sim 5380\ \mathrm{cm}^2/\mathrm{V\,s}$ at 77 K with a total sheet carrier density of $\sim 9\times 10^{13}\ \mathrm{cm}^{-2}$, indicating the presence of multiple layers of high-mobility 2DEGs, as can be expected due to the very strong polarization. For the rest of the letter, we discuss the single AlN/GaN heterojunctions.

The misfit strain in an AlN layer coherently strained on GaN is $\epsilon \sim 2.4\%$. Using a simple (Blanc's) estimate for the critical thickness of AlN on GaN, one gets $t_{cr} \sim b_e/2\epsilon \sim 6.5$ nm (here, $b_e = 0.3189$ nm is the length of the Burgers vector).[14] Figure 1 shows the surface morphologies of the AlN surface around this expected critical thickness as measured by atomic force microscopy (AFM). For $t = 1-6$ nm, the surfaces are smooth (rms roughness $\leqslant 0.4$ nm) and exhibit atomic steps, indicating high-quality growth. Faintly discernible cracks appear for $t \sim 7$ nm, whereas very clearly resolved cracks along the hexagonal $[11\bar{2}0]$ axes are seen for $t = 8$ nm. Each crack line can be observed to intersect with a

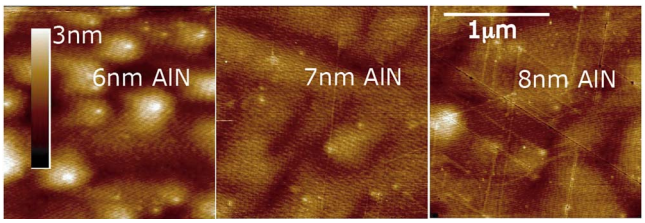

FIG. 1. (Color online) AFM images showing $2\times 2\ \mu\mathrm{m}^2$ scans of the AlN surfaces after growth.

[a]Electronic mail: ycao1@nd.edu

 © 2007 American Institute of Physics
Downloaded 02 May 2007 to 129.74.160.64. Redistribution subject to AIP license or copyright, see http://apl.aip.org/apl/copyright.jsp

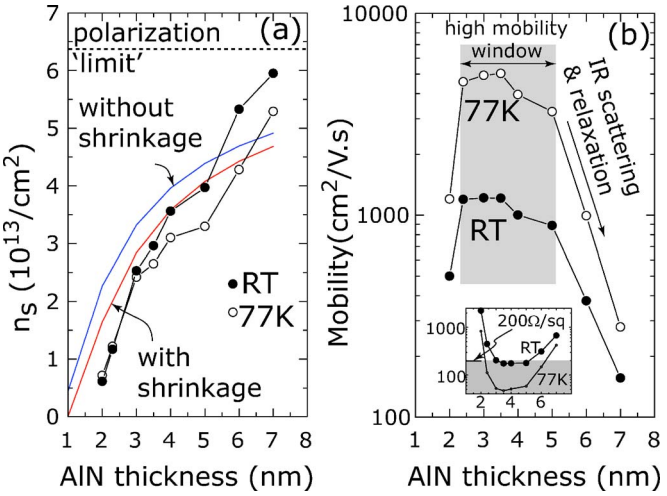

FIG. 2. (Color online) (a) Dependence of the 2DEG density measured at room temperature and 77 K on the AlN thickness, along with calculated curves considering strain-induced band gap shrinkage (red line) and band-gap-shrinkage-free AlN (blue line); (b) mobilities measured at room temperature and 77 K with different AlN thicknesses. Inset: variation of sheet resistance with AlN thickness from 2.0 to 7.0 nm.

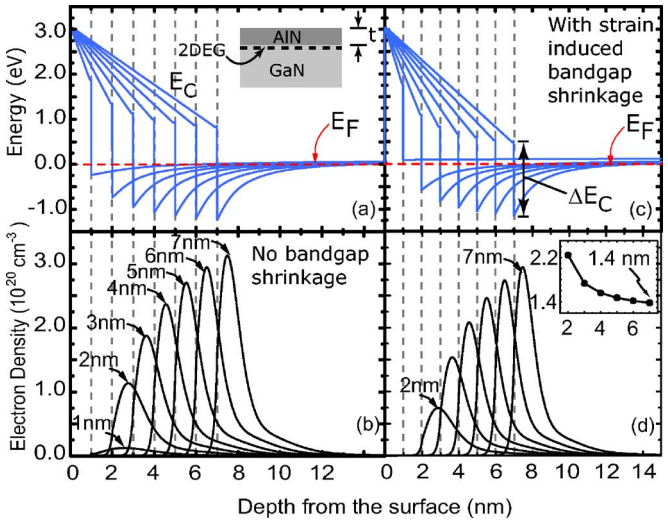

FIG. 3. (Color online) Self-consistent Poisson-Schrödinger simulation for band diagram and 2DEG distributions at the AlN/GaN heterojunctions: the band gap of AlN used in (a) and (b) is the complete unstrained gap (6.2 eV), whereas for (c) and (d), the band gap shrinkage due to biaxial strain is taken into account. Inset: plot of the distance (in nm) between the centroid of the 2DEG distribution and the AlN/GaN interface as a function of the AlN thickness (in nm). (c) and (d) can much better explain the experimental data in Figure 2(a).

bright spot in the AFM image, indicating that the cracks nucleate at the tips of threading dislocations and propagate along a cleavage plane. For the rest of this work, the discussion would be limited to the electronic properties of AlN/GaN with $t \leqslant 7$ nm. The effect of strain relaxation on the mobility of the 2DEG electrons is rather severe, as is presented later in this work.

Ohmic contacts were formed for the AlN/GaN heterojunctions in the van der Pauw geometry. Hall measurements were performed for all the samples at room temperature and at 77 K. The results are shown in Fig. 2. The 77 K 2DEG charge sheet density increases from $\sim 5 \times 10^{12}$/cm^2 to $\sim 5.5 \times 10^{13}$/cm^2 as the AlN barrier thickness is increased from $t=2$ to 7 nm. The measured sheet density approaches the highest density possible due to the difference in the (spontaneous + piezoelectric) polarization between AlN and GaN at large AlN thicknesses close to the critical thickness, as shown in Fig. 2(a). The measured RT electron mobility is ~ 1200 cm^2/V s for AlN thicknesses between 2.4 and 4.0 nm and decreases at both smaller and larger values, as shown in Fig. 2(b). The 77 K mobility is higher than ~ 5000 cm^2/V s for the same samples that exhibit high RT mobility. The 3.5 nm AlN sample gave mobilities of 1213 cm^2/V s at room temperature and 5032 cm^2/V s at 77 K. The effective sheet resistance for the 2DEGs in this "high-mobility window" is lower than 200 Ω/□, in the range of 170 Ω/□, as shown in the inset. These are the *lowest* sheet resistances reported to date in the III-V nitride system and can prove to be highly attractive for the reduction of parasitic resistances in high-speed HEMT design. The measured electronic and transport properties of these very high-conductivity 2DEGs are analyzed using theoretical models and further transport measurements in the rest of this letter.

The electronic properties of the heterostructures were modeled using a self-consistent Poisson-Schrödinger solver.[15] The conduction band diagrams for various AlN thicknesses are shown in Figs. 3(a)–3(d), along with the 2DEG spatial distribution. For metal-AlN Schottky, barrier heights around 3 eV have been reported in the literature both theoretically and experimentally.[16–18] A free-surface barrier height of 3.0 eV was used in the calculation, since we find that a barrier height less than 2 eV results in much higher sheet densities than what we measure. When the AlN thickness increases, the triangular quantum well at the heterojunction becomes deeper with respect to the Fermi level due to the polarization-induced electric field in the barrier. The 2DEG density increases as a result. However, the spread of the electron distribution gets narrower with increasing density, and the electron gas is electrostatically pushed closer to the AlN/GaN interface. It should also be pointed out that using the conduction band offset between *unstrained* AlN and GaN ($\Delta E_C = 2.1$ eV) in the model systematically overestimates the 2DEG sheet density, as shown in Fig. 2(a). Since the pseudomorphic AlN layer experiences a biaxial tensile strain, the band gap shrinks, as does the conduction band offset. By using the reduced conduction band offset via the deformation potential of AlN,[19] the self-consistent theoretical model can much better account for the measured sheet densities, as shown in Figs. 3(c), 3(d), and 2(a). The sheet density increases at the onset of relaxation of the AlN layer. This may be partially attributed to the increase in the band offset due to the removal of strain or nonlinear polarization coefficients.[20] However, the relaxation of AlN also leads to a loss of the piezoelectric charge; therefore, more analysis is necessary to explain this phenomenon.

The transport properties of the high-density 2DEGs are plotted in Fig. 4. Part (a) shows the RT and 77 K mobilities as a function of the 2DEG sheet density. Along with the mobility data reported in this work, the highest mobilities reported earlier in AlN/GaN heterojunctions by Smorchkova *et al.*[8] are also shown for comparison. The drop in the mobility for the lowest sheet density samples is possibly due to strong remote Coulombic scattering from charged surface states, since the AlN thickness for this structure is only 2 nm. Coulombic scattering is exacerbated by the weak screening by the low sheet density. However, the decrease in mobility

Downloaded 02 May 2007 to 129.74.160.64. Redistribution subject to AIP license or copyright, see http://apl.aip.org/apl/copyright.jsp

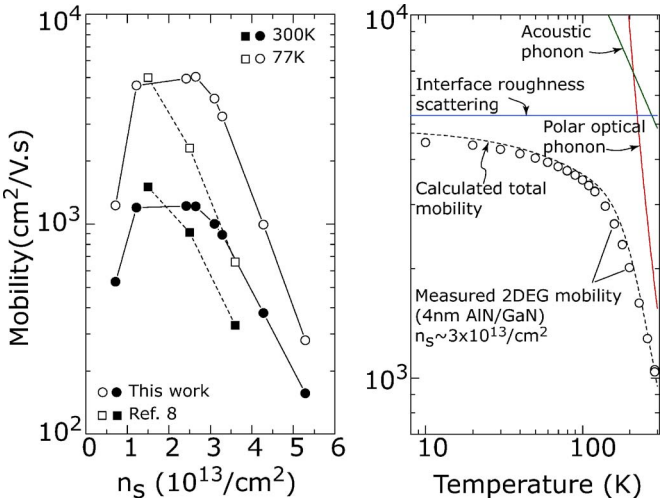

FIG. 4. (Color online) (a) Variation of mobility with 2DEG density in our work (circles), compared with that in Ref. 8 (squares); (b) temperature-dependent Hall data of single AlN/GaN heterojunction with the thickness of 4.0 nm (circles). With the theoretical transport model, mobility is found to be limited by IR scattering at low temperature and polar optical phonons at high temperature.

for the high sheet density samples defines the limits of the maximum RT conductivities attainable in III-V nitride heterostructures. If the scattering mechanisms that are dominant for high-density 2DEGs can be identified, it will guide the modifications to the growth and/or the layer structure that will be necessary to improve the conductivity further. To precisely determine the scattering processes that result in such behavior, temperature-dependent Hall measurements were performed for the 4 nm AlN/GaN heterojunction. The Hall measurements were performed by loading the sample into a closed-cycle He cryostat, and the temperature was varied between 10 and 300 K. The experimental results are shown in Fig. 4(b), along with the results of a theoretical model.

The mobility increases monotonically as temperature is lowered, which is the signature of absence of strong Coulombic scattering. Coulombic scattering can occur due to charged dislocations ($N_{\mathrm{dis}} \sim 10^9/\mathrm{cm}^2$), remote (surface) charged states ($n_{\mathrm{surf}} \sim n_s$ by charge neutrality), and background charged impurities ($N_{\mathrm{back}} \sim 10^{16}/\mathrm{cm}^2$). All these scattering events were included in the model but were found to be much weaker and insignificant than those that are shown in the figure. At room temperature, expectedly, scattering from polar optical phonons dominates over all other scattering mechanisms in a reasonably clean 2DEG. Since alloy scattering is forbidden in an all-binary AlN/GaN heterojunction, interface roughness (IR) scattering is found to be dominant at low temperatures. The theoretical model used here assumes a roughness of 0.25 nm in the growth direction corresponding to half a unit cell and 1.25 nm in the lateral direction; these numbers are found to be characteristic of most III-V nitride heterojunctions[21] and can describe the measured mobility data reasonably well. As the inserted plot in Fig. 3(d) shows, the thicker the AlN barrier, the closer the centroid of the electron distribution shifts to the interface. This implies that a thicker AlN leads to a more severe IR scattering. The calculated 2DEG distribution in Fig. 3(d) can be used to describe the measured degradation of mobility at high sheet densities [Fig. 4(a)] quantitatively. Such a treatment is deferred to a later work. As the AlN barrier reaches its critical thickness, additional scattering sources are created due to strain relaxation. The major conclusion from the theoretical model is that if the growth conditions can be modified to reduce the roughness of the AlN/GaN interface, even higher electron mobilities are possible in the narrow high-mobility window found here.

In conclusion, a high-mobility window for all-binary AlN/GaN heterojunction 2DEGs is observed. Record low sheet resistances are found in these heterostructures, and the primary scattering mechanisms limiting the conductivity are identified as due to structural defects due to interface roughness, strain relaxation, and polar optical phonon scattering.

The authors would like to acknowledge financial support from the Office of Naval Research (Colin Wood) and DARPA (M. Rosker) for this work.

[1] L. Shen, S. Heikman, B. Moran, R. Coffie, N.-Q. Zhang, D. Buttari, I. P. Smorchkova, S. Keller, S. P. DenBaars, and U. K. Mishra, IEEE Electron Device Lett. **22**, 457 (2001).
[2] M. Gonschorek, J.-F. Carlin, E. Feltin, M. A. Py, and N. Grandjean, Appl. Phys. Lett. **89**, 062106 (2006).
[3] H. Kawai, M. Hara, F. Nakamura, and S. Imanaga, Electron. Lett. **34**, 592 (1998).
[4] E. Alekseev, A. Eisenbach, and D. Pavlidis, Electron. Lett. **35**, 2145 (1999).
[5] M. Higashiwaki, T. Mimura, and T. Matsui, IEEE Electron Device Lett. **27**, 719 (2006).
[6] D. Hofstetter, E. Baumann, F. R. Giorgetta, M. Graf, M. Maier, F. Guillot, E. Bellet-Amalric, and E. Monroy, Appl. Phys. Lett. **88**, 121112 (2006).
[7] S. C. Binari, K. Doverspike, G. Kelner, H. B. Dietrich, and A. E. Wickenden, Solid-State Electron. **41**, 177 (1997).
[8] I. P. Smorchkova, S. Keller, S. Heikman, C. R. Elsass, B. Heying, P. Fini, J. Speck, and U. K. Mishra, Appl. Phys. Lett. **77**, 3998 (2000).
[9] I. P. Smorchkova, L. Chen, T. Mates, L. Shen, S. Heikman, B. Moran, S. Keller, S. P. Den-Baars, J. Speck, and U. K. Mishra, Appl. Phys. Lett. **90**, 5196 (2001).
[10] A. Bourret, C. Adelmann, B. Daudin, J. Rouviere, G. Feuillet, and G. Mula, Phys. Rev. B **63**, 245307 (2001).
[11] A. M. Sanchez, F. J. Pacheco, S. I. Molina, J. Stemmer, J. Aderhold, and J. Graul, J. Electron. Mater. **30**, L17 (2001).
[12] K. Jeganathan, T. Ide, M. Shimizu, and H. Okumura, Appl. Phys. Lett. **93**, 2047 (2006).
[13] T. Koyama, M. Sugawara, Y. Uchinuma, J. F. Kaeding, R. Sharma, T. Onuma, S. Nakamura, and S. F. Chichibu, Phys. Status Solidi A **203**, 1603 (2006).
[14] J. Singh, *Physics of Semiconductors and Their Heterostructures* (McGraw-Hill, New York, 1992), p. 734.
[15] I. H. Tan, G. L. Snider, L. D. Chang, and E. L. Hu, J. Appl. Phys. **68**, 4071 (1990).
[16] M. W. Wang, J. O. McCaldin, J. F. Swenberg, T. C. McGill, and R. J. Hauenstein, Appl. Phys. Lett. **66**, 1974 (1995).
[17] D. Qiao, L. S. Yu, S. S. Lau, J. M. Redwing, J. Y. Lin, and H. X. Jiang, J. Appl. Phys. **87**, 801 (2000).
[18] Chris G. Van de Walle and J. Neugebauer, Nature (London) **423**, 626 (2003).
[19] B. K. Ridley, W. J. Schaff, and L. F. Eastman, J. Appl. Phys. **94**, 3972 (2003).
[20] F. Bernardini and V. Fiorentini, Phys. Rev. B **64**, 085207 (2001).
[21] Y. Zhang, I. P. Smorchkova, C. R. Elsass, S. Keller, J. P. Ibbetson, S. Denbaars, U. K. Mishra, and J. Singh, J. Appl. Phys. **87**, 7981 (2000).

Downloaded 02 May 2007 to 129.74.160.64. Redistribution subject to AIP license or copyright, see http://apl.aip.org/apl/copyright.jsp